Preprint version of:
Perez, M., Suarez, A., Heredia, G. and Ollero, A. Positioning System for Pipe Inspection with Aerial Robots using Time of Flight Sensors. 4th Iberian Robotics Conference (ROBOT 2019), Springer, Cham

Positioning System for Pipe Inspection with Aerial Robots using Time of Flight Sensors

Manuel Perez[1], Alejandro Suarez[1], Guillermo Heredia[1] and Anibal Ollero[1]

[1] GRVC Robotics Labs Seville, School of Engineers of Seville, Spain
{asuarezfm, guiller, aollero}@springer.com

Abstract. This paper describes a positioning system for aerial robots consisting of a linear array of time-of-flight (ToF) sensors whose orientation angle is controlled with micro servo, allowing the detection and accurate localization of the contour of a pipe to be inspected. The system, integrated in a hexarotor vehicle, has three operation modes: searching, aligning, and tracking. In the first phase, a scan motion is conducted rotating the servo in a wide range until one of the four ToF sensors of the array detects a close obstacle. Then, the rotation angle is adjusted to align the array with the normal vector of the surface, tracking actively its contour while providing an estimation of the relative position and orientation. The paper details the design and implementation of the system, the control scheme, the position estimator, and its integration in an aerial robot. Experimental results carried out in test-bench show the performance of the system.

Keywords: Aerial Robotic Inspection, Time-of-Flight Sensor, Position Sensor.

1 Introduction

The ability of aerial robots to reach quickly high altitude or distant workspaces results of interest for a wide variety of inspection and maintenance operations in industrial facilities, conducted nowadays by human operators in risky conditions. Motivated by the convenience to reduce the time, cost and resources involved in these operations, the aerial manipulation field [1] proposes the integration of control, perception and planning capabilities in aerial platforms equipped with robotic arms. The installation and retrieval of inspection tools [2], the inspection by contact [3][4], the inspection of power lines [5], or the cleaning of wind turbines [6] are some illustrative examples of applications that may benefit from this technology. Several prototypes of aerial robots have been developed in recent years, integrating single arm [7][8] or dual arm [2][9] manipulators in multirotor platforms, demonstrating the grasping objects [2] and control the contact forces [10].

In the execution of an aerial manipulation mission, it is possible to identify three phases: navigation through the environment, approaching to the workspace, and realization of the particular operation. Real-Time Kinematics (RTK) Global Positioning System (GPS), vision-based [11] and range-only [12] Simultaneous Localization and Mapping (SLAM), or laser tracking systems [13] have been used for the position and

trajectory control of multirotor vehicles in outdoors. However, higher positioning accuracies are needed once the aerial robot is close to the workspace and operating on flight, taking into account that the reach of the manipulator is relatively small (around 50 cm). ARUCo tags have been extensively used in indoors and outdoors [14], although the use of these markers and the computational resources may limit their application. A docking system is proposed in [15] for measuring the relative position of the aerial platform using a robotic arm attached to fixed point over a pipe. A cooperative virtual sensor is built in [16] exploiting the vision sensors on-board a group of quadrotors (observers) for estimating the position and velocity of a target quadrotor.

In our previous work we developed several prototypes of lightweight and compliant aerial manipulation robots [17] intended for inspection and maintenance of pipe structures in chemical plants [1]. The need of a high accuracy positioning system was evidenced in the grasping and installation of inspection devices on flight [2], taking into account that the effective reach of a human-size manipulator (w.r.t. the nominal operation position) is around 30 cm. Reference [9] analyzes the limitations in the performance of the manipulator due to the motion constraints and dynamic coupling with the aerial platform. The ARUCo markers were employed in [10] to measure the position of the aerial manipulator relative to the inspection point, although the detection of the marker was affected by shades and changes in the illumination. The long reach aerial manipulator presented in [18] introduced a time of flight sensor attached at the end effector to measure the distance to a pipe, enhancing the situational awareness of the human operator.

The main contribution of this work is the design and development of a positioning system based on Time of Flight (ToF) sensors to be used in the inspection of high altitude pipe structures with aerial manipulation robots. The system consists of two linear arrays of distance sensors whose orientation angle is controlled to track the contour of the pipe, providing an estimation of the relative position and orientation. The paper details the mechanical design and integration in a hexarotor platform, the electronics of the system, the operation modes for the detection and tracking of close surfaces, as well as the geometric relationships used for estimating the relative pose. Each linear array consist of four VL53L0 SATEL sensors manufactured by ST Microelectronics (2100 mm max distance, 20 – 50 Hz update rate, 3 grams weight), using a micro servo to control its orientation in the pitch angle. Known this angle and the mean distance to the obstacle, it is possible to estimate the position in the two orthogonal axes (XZ). A second array is used to estimate the relative orientation, what can be useful for landing the aerial platform over the pipes. Experimental results conducted in an indoor test bench evaluate the performance of these sensors and the positioning system, paying special attention to the accuracy and update rate. The rest of the paper is organized as follows. Section 2 describes the positioning system, including the mechanical design, electronics, and its integration in a hexarotor platform. Section 3 explains the three operation modes (searching-aligning-tracking) of the sensor and the control of the orientation angle, whereas Section 4 describes the relative position estimator. The experimental results are presented in Section 5, summarizing the conclusions and future work in Section 6.

2 System description

2.1 Mechanical construction and sensor specifications

The prototype presented in this work and shown in **Fig. 1** implements a laser tracking system capable to estimate the position and orientation of a multirotor with respect to a pipe or a flat surface at distances below 2 meters. It consists of two moving arrays of four VL53L0X-SATEL time of flight sensor boards whose main specifications are summarized in **Table 1**. These devices, manufactured by ST Microelectronics, rely in the time taken by a laser pulse to hit the target and return to estimate the distance. The orientation of each array is controlled with a Pololu micro metal gear motor 250:1 and a DRV 8833 driver, measuring the rotation angle of the motor shaft with a Murata SV01A potentiometer. Known the distance measured by the array and its orientation angle, it is possible to obtain the position of an obstacle in the forward and vertical directions (XZ- axes). Combining the measurements provided by two arrays it is possible to obtain the relative orientation in the yaw angle with respect to the obstacle, as it will be seen in Section 4. This may be useful to control the position and orientation of the aerial robot relative to a pipe during the realization of the inspection operation or for landing the aerial platform.

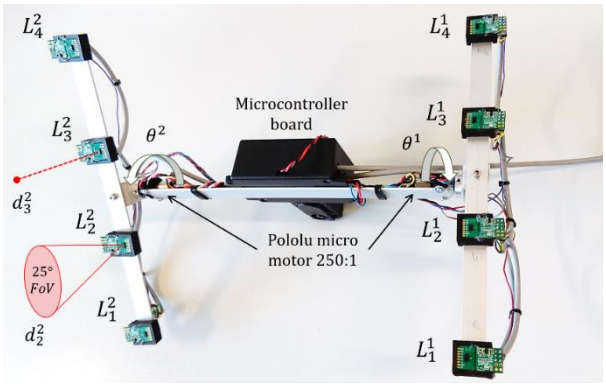

Fig. 1. Positioning system with two arrays of four time of flight sensors.

Table 1. Main specifications of the VL53L0X-SATEL time of flight sensor board.

Size / Weight	31 × 26,5 × 6,5 mm / 318,2 grams (total)
Ranging time	30 – 200 ms (depending on distance)
Max. ranging (17% grey)	80 cm (Indoor) – 50 cm (Outdoor)
Max. ranging (88% white)	+200 cm (Indoor) – 80 cm (Outdoor)
Ranging accuracy	4 – 7% (Indoor) – 6 – 12% (Outdoor)
Field of View	35° (Emitter) – 25° (Collector)

2.2. Electronics and hardware architecture

The positioning system is implemented in a STM32F103 microcontroller that features all the peripherals required for interfacing the sensors and for controlling the DC micro servos: two I2C buses (one per array) to read the VL53L0X sensors, one UART for sending the estimated pose to the main computer board, two ADC channels to get the rotation angle of the micro servos, and four PWM signals to control the two motor drivers. A picture of the components and the architecture of the positioning system is shown in **Fig 2**. Each array of sensors is connected to an independent I2C bus for simplifying the wiring and increasing the read rate. A pair of Pololu micro metal gear motors 250:1 are used to rotate the arrays in the pitch angle during the searching, aligning and tracking phases. The DRV 8833 driver allows the microcontroller to vary the rotational speed and the direction of the servos through the PWM signals, using the ADC to get position feedback. The whole system is powered by a 2S LiPo battery, exploiting the voltage regulator embedded in the microcontroller board. Communication with main computer is done using a custom protocol over full duplex UART.

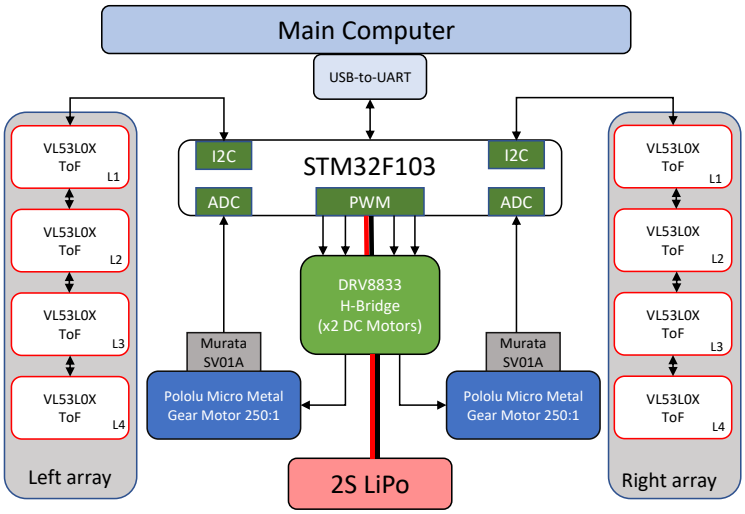

Fig. 2. Hardware architecture and components of the positioning system.

2.3. Geometric model

The geometric model of a single array of sensors is illustrated in **Fig. 3**, considering its application for the relative localization of pipes. Here d_j^i is the distance measured by the j-th sensor of the i-th array, with $i = \{1, 2\}$, $j = \{1, 2, 3, 4\}$, θ^i is the rotation angle of the corresponding array, Δx is the separation distance between lasers whereas D_{pipe} is the diameter of the pipe to be inspected. It is imposed that $\Delta x \sim 0.8 \cdot D_{pipe}$ to ensure that the contour of the pipe is tracked by two laser sensors, otherwise the aligning phase described in Section 3 will fail.

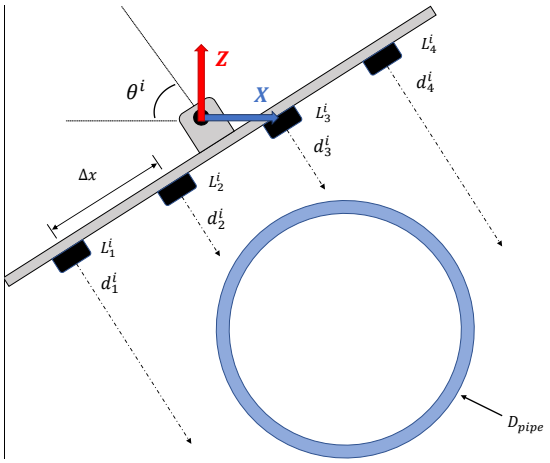

Fig. 3. Geometric model of an array of sensors tracking the contour of a pipe.

The local XZ-axes of the positioning system are also represented in **Fig. 3**. For simplicity, it is assumed that the origin is at the midpoint of the array, coinciding with the axis of rotation of the micro motor. In the experimental results presented in **Section 5.2** and **5.3**, the angle $\theta^i = 0$ corresponds to the array pointing downwards.

2.4. Integration in hexarotor platform

The positioning system with two arrays of ToF sensors has been integrated in a S550 hexarotor platform, as illustrated in **Fig. 4**. An L-shaped aluminum frame (30 × 2 mm section) is used to attach the sensor case with the base of the multirotor in such a way that the arrays do not interfere with the propellers or the landing gear.

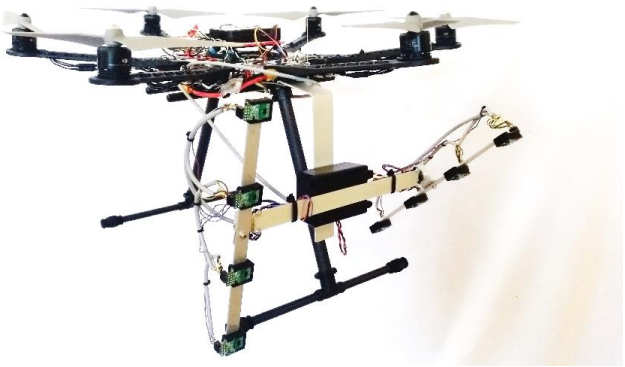

Fig. 4. Positioning system integrated in a hexarotor platform.

3 Operation modes and control

The positioning system implements three operation modes in the microcontroller board according to the state machine represented in **Fig. 5**: searching, aligning, and tracking. A sequence of pictures illustrating the performance of the developed prototype can be seen in **Section 5.2**. In the following, it is assumed that the positioning system is integrated in a multirotor platform, which is approaching to a pipe structure to be inspected. The obstacles are initially far away, out of the range of the sensors, so the searching mode is firstly executed. In this mode, the two arrays perform a scan motion rotating the micro motors in a wide range (±100°) at constant speed (~60 °/s), trying to find close obstacles. If one of the external lasers (d_1^i or d_4^i) hits the incoming pipe, the system enters in the aligning mode in which the array is rotated quickly towards the direction of the obstacle until this is detected by the internal sensors (d_2^i or d_3^i). In this phase, the microcontroller acts over the motor to align the measurement of both sensors ($d_2^i = d_3^i$) in order to ensure that the array is oriented orthogonally to the normal vector of surface of the pipe (see **Fig. 3**). Note that the circular profile of the pipe facilitates the detection and tracking of its contour.

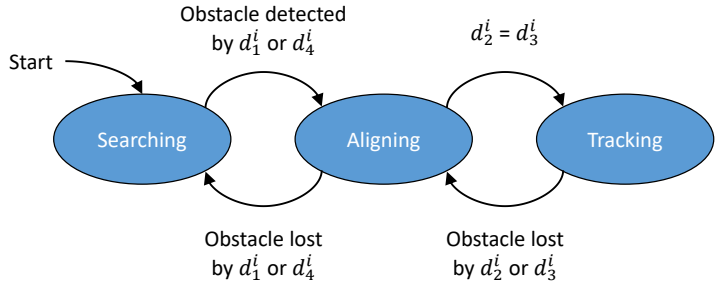

Fig. 5. State machine representing the three operation modes and transitions of the system.

The orientation of each array is controlled generating the following reference at 30 Hz in such a way that the measurements of the inner sensors are equal:

$$\theta_{ref}^i = \theta^i + k \cdot \left(d_2^i - d_3^i\right) \tag{1}$$

Here θ^i and θ_{ref}^i, are the current and reference orientation of the i-th array, and k is the proportional gain of the controller. This reference is taken as input by a low level PID position controller that acts over the PWM signal of the motor driver:

$$pwm^i = K_P \theta_e^i + K_I \int_0^t \theta_e^i d\tau + K_D \dot{\theta}_e^i \tag{2}$$

Here $pwm^i \in [-1, 1]$ is the normalized PWM signal, $\theta_e = \theta_{ref} - \theta$ is the angular error, whereas K_P, K_I and K_D are the proportional, integral and derivative gains of the

position controller, respectively, which is executed at 200 Hz. **Fig. 6** shows the complete control scheme.

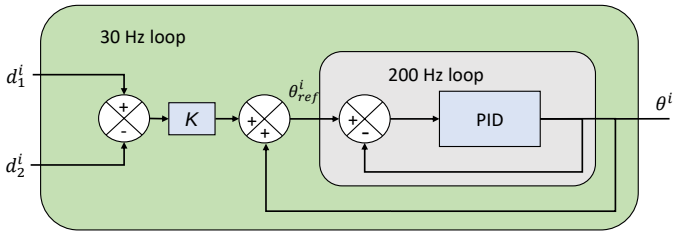

Fig. 6. Low level controller of the positioning system used in the tracking mode: inner PID position control loop and outer proportional controller used for aligning the internal sensors.

Once the aligning phase is complete ($d_2^i = d_3^i$), the low level controller will keep active the tracking of the contour of the pipe while the relative position of the aerial platform w.r.t. the pipe is computed and sent to the main computer board at 30 Hz, as it will be described in next section. The position deviations in the multirotor due to wind perturbations or physical interactions will be compensated controlling the orientation angle of the array. If the measurement of one of the inner sensors (L_2 or L_3) goes suddenly out of range, the system will automatically switch to the aligning mode to recover the tracking of the pipe. In case the measurement of the four sensors of the array go out of range, the system will enter in searching mode to redetect the pipe.

4 Relative position estimation

As indicated in the introduction, the motivation of this work is the development of a high accuracy positioning system intended for an aerial robot operating close to pipes, where the distances are relatively small (below one meter). The proposed system uses ToF sensors to obtain the distance to the surface of the obstacle, and a potentiometer to measure the rotation angle of the array. Taking into account the diagram depicted in **Fig. 3**, the position of the obstacle relative to the rotation axis of the motor can be estimated as follows:

$$x^i \cong \frac{\left(d_2^i + d_3^i\right)}{2} \cdot sin(\theta) \tag{3}$$

$$z^i \cong \frac{\left(d_2^i + d_3^i\right)}{2} \cdot cos(\theta) \tag{4}$$

Note that the approximation in Eq. (3) and (4) neglects the curvature of the pipe and considers the mean distance of the inner sensors. According to the datasheet of the VL53L0X sensor (see specifications in **Table 1**), the field of view of the collector is 25°, so the measured distance will correspond to closest point within the reception cone, in this case, the curved surface between the two inner sensors.

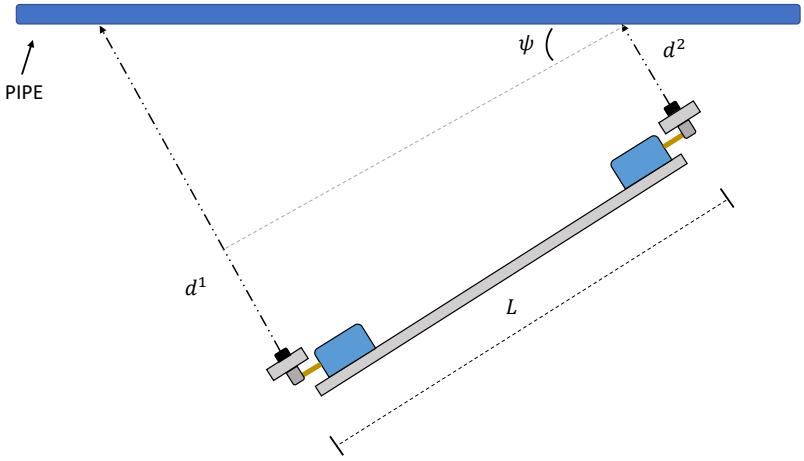

Fig. 7. Estimation of the orientation (yaw angle) of the positioning system relative to a pipe from the distance measured by both arrays.

Let us consider now the double-array positioning system depicted in **Fig. 7**, where L is the baseline between the left and right arrays, the orientation angle in the horizontal plane (yaw) relative to a target pipe is denoted by ψ, whereas d^i and θ^i represent the distance measured by each array and its corresponding rotation angle respectively, with, $i = \{1, 2\}$. The orientation of the baseline can be obtained geometrically from the projection in the XY-plane of the distances measured by each array as follows:

$$\psi = \tan^{-1}\left(\frac{d^1 sin(\theta^1) - d^2 sin(\theta^2)}{L}\right) \tag{5}$$

Here $d^i sin(\theta^i)$ represents the projection of the distance measured by the i-th array over the XY-plane, so the difference between both arrays corresponds to the length of the leg in the formed triangle. Note that the direction of the laser beam is orthogonal to the baseline of the pair of arrays.

It is necessary to highlight that the pose estimation given by Equations (3) – (5) is obtained assuming that the positioning system remains almost horizontal during the tracking phase, since the multirotor platform usually operates in hovering conditions.

5 Experimental Results

5.1 ToF Sensor Characterization

In order to provide a high accuracy positioning estimation, it is necessary to conduct a calibration process to determine the deviation in the position measurement given by the sensor with respect to a ground truth. **Fig. 8-left** represents the measurements given by

the VL53L0X sensor along with the real value obtained from a ruler, whereas **Fig. 8-right** shows the calibrated signal obtained applying a simple correction curve. **Table 2** indicates the mean error and standard deviation for some representative distances.

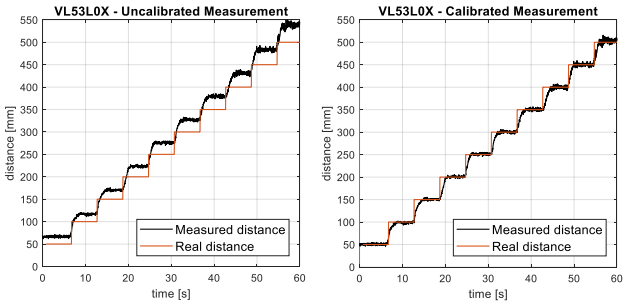

Fig. 8. Positioning accuracy of the VL53L0X-SATEL ToF sensor: uncalibrated (left) and calibrated (right) with offset correction. A 50 cm ruler is used as ground truth.

Table 2. Data obtained from sensor before and after calibration.

	Uncalibrated			Calibrated		
Ground truth	Measurement	Error	STD	Measurement	Error	STD
100	117,2	17,2	1,7	99,1	-0,9	1,6
200	223,3	23,3	1,8	200,8	0,8	1,8
300	326,6	26,6	2,8	299,8	-0,2	2,7
400	431,3	31,3	3,7	400,1	0,1	3,5
500	539	39	4,3	503,3	3,3	4,0

5.2 Detection and Position Estimation of Pipe Contour

The goal of this experiment is to evaluate the performance of the developed positioning system estimating the relative position of a pipe with respect to the local axes shown in **Fig. 3**. The experiment, conducted in an indoor testbed, consists of moving the baseline of the array along the X and Z axes following the contour of a 200 mm Ø PVC pipe while the system is in tracking mode. **Fig. 9** and **Fig. 10** represent the estimated position given by Equation (3) and (4) along with the mean distance given by the inner sensors and the rotation angle of each array. The execution of the experiment can be followed in the sequence of pictures illustrated in **Fig. 11**. The estimation is obtained directly without applying any filter to the signal provided by the sensors. The mechanical clearance of the micro motors introduces additional noise in the estimation.

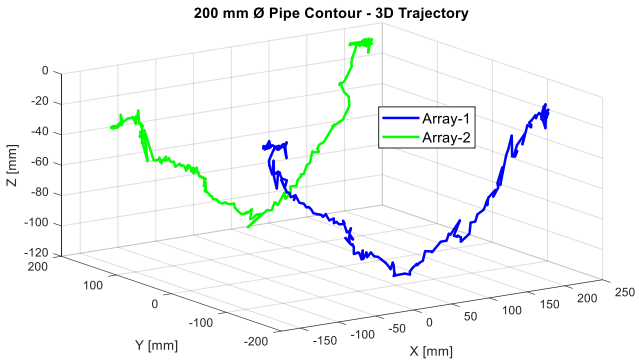

Fig. 9. 3D position estimation corresponding to the contour of the 200 mm Ø pipe.

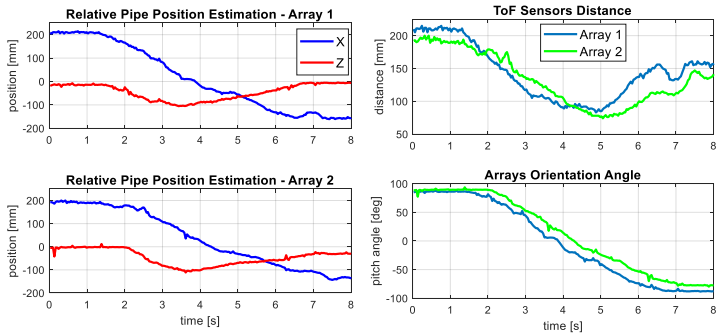

Fig. 10. Evolution of the relative position estimation provided by both arrays (left). Mean distance and orientation angle of the arrays (right).

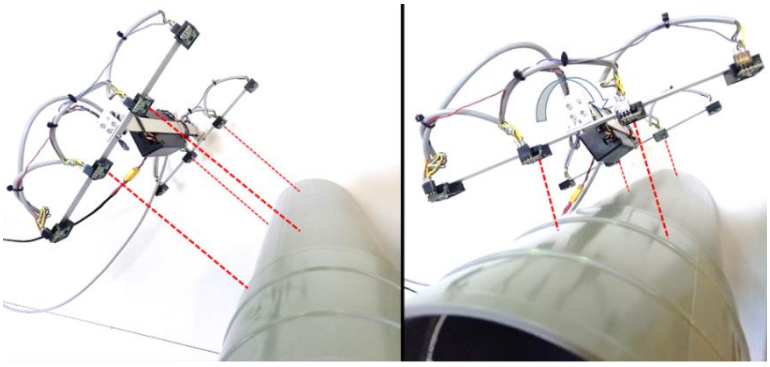

Fig. 11. Two poses of the positioning system while tracking the contour of the pipe.

5.3 Relative Orientation Estimation

In this experiment, the baseline of the positioning system is rotated in the yaw angle with respect to the pipe, maintaining fixed the relative position. **Fig. 12** represents the estimation given by Eq. (5) along with the distance and rotation angle of both arrays.

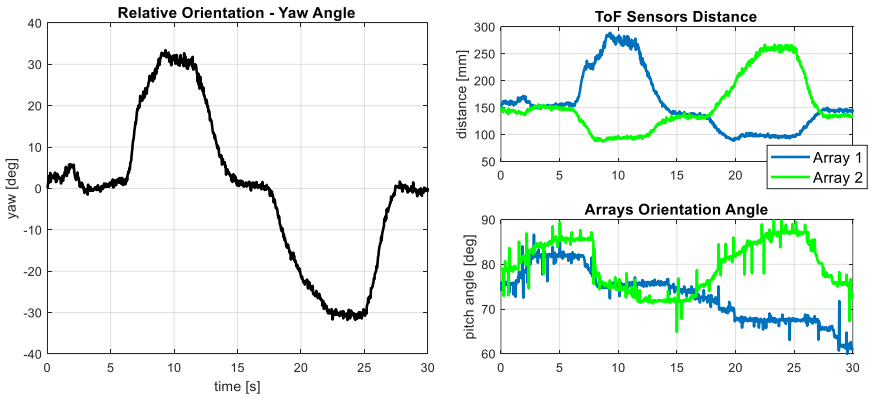

Fig. 12. Estimation of the relative orientation of the pipe in the yaw angle.

6 Conclusion

This paper described the design of a positioning system consisting of two orientable arrays of time of flight (ToF) sensors, used to estimate the relative position and orientation of a pipe to be inspected with an aerial robot. Each array counts with four sensors and a micro servo actuator that actively tracks the contour of the pipe, being able to detect and recover from losses. Besides their low weight, these devices provide highly accurate (< 1 cm) distance measurements within a range around 2 m, and update rates above 30 Hz. Unlike vision sensors, which typically require a certain degree of texture to reconstruct the shape of a surface, the measurement obtained from the laser pulse does not depend on the target reflectance. However, the sunlight has a significant influence over the operation range and accuracy, what limits its application in outdoor scenarios.

Acknowledgments

This work was supported by the HYFLIERS (H2020-2018-779411) project, funded by the European Commission, and the ARM-EXTEND (DPI2017-89790-R) and ARTIC (RTI2018-10224-B-I00) projects, funded by the Spanish MINECO.

References

1. Ollero, A., *et al*.: The AEROARMS project: aerial robots with advanced manipulation capabilities for inspection and maintenance. In *IEEE Robotics & Automation Magazine*, vol. 25, no. 4, pp. 12-23, (2018).
2. Suarez, A., Heredia, G., Ollero, A.: Design of an anthropomorphic, compliant, and lightweight dual arm for aerial manipulation. In *IEEE Access*, vol. 6, pp. 29173-29189, (2018).
3. Trujillo, M. Á., Martínez-de Dios, J. R., Martín, C., Viguria, A., Ollero, A.: Novel aerial manipulator for accurate and robust industrial NDT contact inspection: a new tool for the oil and gas inspection industry. In *Sensors (Basel, Switzerland)*, *19*(6), 1305, (2019).
4. Bartelds, T., Capra, A., Hamaza, S., Stramigioli, S. and Fumagalli, M.: Compliant aerial manipulators: toward a new generation of aerial robotic workers. In *IEEE Robotics and Automation Letters*, vol. 1, no. 1, pp. 477-483, (2016).
5. Deng, C., Wang, S., Huang, Z., Tan, Z., Liu, J.: Unmanned aerial vehicles for power line inspection: a cooperative way in platforms and communications. In Journal of Communications, 9, pp. 687-692
6. AERONES homepage, https://aerones.com/eng/wind_turbine_maintenance_drone/, last accessed 2019/05/28.
7. Cano, R., Pérez, C., Pruano, F., Ollero, A., Heredia, G.: Mechanical design of a 6-DOF aerial manipulator for assembling structures using UAVs. In 2nd RED-UAS workshop on research, education and development of unmanned aerial systems (2013).
8. Bellicoso, C. D., Buonocore, L. R., Lippiello, V., Siciliano, B.: Design, modeling and control of a 5-DoF light-weight robot arm for aerial manipulation. In 3rd Mediterranean Conference on Control and Automation (MED), pp. 853-858, Torremolinos (2015).
9. Suarez, A., Jimenez-Cano, A. E., Vega, V., Heredia, G., Rodriguez-Castaño, A., Ollero, A.: Design of a lightweight dual arm system for aerial manipulation. In Mechatronics, Vol. 50, pp. 30-44, (2018).
10. Suarez, A., Heredia, G., Ollero, A.: Physical-virtual impedance control in ultralightweight and compliant dual-arm aerial manipulators. In *IEEE Robotics and Automation Letters*, vol. 3, no. 3, pp. 2553-2560, (2018).
11. Artieda, J., Sebastian, J. M., Campoy, P., Correa, J. F., Mondragón, I. F., Martínez, C., Olivares, M.: Visual 3-d slam from UAVs. In *Journal of Intelligent and Robotic Systems*, *55* (4-5), 299, (2009).
12. Torres-Gonzalez, A., Martinez-de-Dios, J. R., Ollero, A.: Range-only SLAM for robot-sensor network cooperation. In Autonomous Robots, vol. 42(3), pp. 649-663, (2018).
13. Huh, S., Shim, D. H., Kim, J.: Integrated navigation system using camera and gimbaled laser scanner for indoor and outdoor autonomous flight of UAVs. In *IEEE/RSJ International Conference on Intelligent Robots and Systems*, Tokyo, 2013, pp. 3158-3163, (2013).
14. Sani, M. F., Karimian, G.: Automatic navigation and landing of an indoor AR. drone quadrotor using ArUco marker and inertial sensors. In *International Conference on Computer and Drone Applications (IConDA)*, pp. 102-107, (2017).
15. Soria, P. R., Arrue, B., Ollero, A.: A 3D-printable docking system for aerial robots: controlling aerial manipulators in outdoor industrial applications. *IEEE Robotics & Automation Magazine*, vol. 26, no. 1, pp. 44-53, (2019).
16. Suarez, A., Heredia, G., Ollero, A.: Cooperative virtual sensor for fault detection and identification in multi-UAV applications. In Journal of Sensors, vol. 2018, Article ID 4515828, 19 pages, (2018).
17. Suarez, A.: Compliant aerial manipulation. PhD Thesis Dissertation, University of Seville (2019).
18. Suarez, A., Sanchez-Cuevas, P., Fernandez, M., Perez, M., Heredia, G. and Ollero, A.: Lightweight and compliant long reach aerial manipulator for inspection operations. In IEEE/RSJ International Conference on Intelligent Robots and Systems (IROS), Madrid, pp. 6746-6752, (2018).